

Yukawa-unified natural supersymmetry

Howard Baer^{1*}, Sabine Kraml^{2†}, Suchita Kulkarni^{2‡}

¹*Dept. of Physics and Astronomy, University of Oklahoma, Norman, OK 73019, USA*

²*Laboratoire de Physique Subatomique et de Cosmologie, UJF Grenoble 1, CNRS/IN2P3, INPG, 53 Avenue des Martyrs, F-38026 Grenoble, France*

Abstract

Previous work on $t - b - \tau$ Yukawa-unified supersymmetry, as expected from SUSY GUT theories based on the gauge group $SO(10)$, tended to have exceedingly large electroweak fine-tuning (EWFT). Here, we examine supersymmetric models where we simultaneously require low EWFT (“natural SUSY”) and a high degree of Yukawa coupling unification, along with a light Higgs scalar with $m_h \sim 125$ GeV. As Yukawa unification requires large $\tan\beta \sim 50$, while EWFT requires rather light third generation squarks and low $\mu \approx 100 - 250$ GeV, B -physics constraints from $\text{BR}(B \rightarrow X_s \gamma)$ and $\text{BR}(B_s \rightarrow \mu^+ \mu^-)$ can be severe. We are able to find models with EWFT $\Delta \lesssim 50 - 100$ (better than 1-2% EWFT) and with Yukawa unification as low as $R_{\text{yuk}} \sim 1.3$ (30% unification) if B -physics constraints are imposed. This may be improved to $R_{\text{yuk}} \sim 1.2$ if additional small flavor violating terms conspire to improve accord with B -constraints. We present several Yukawa-unified natural SUSY (YUNS) benchmark points. LHC searches will be able to access gluinos in the lower 1 – 2 TeV portion of their predicted mass range although much of YUNS parameter space may lie beyond LHC14 reach. If heavy Higgs bosons can be accessed at a high rate, then the rare $H, A \rightarrow \mu^+ \mu^-$ decay might allow a determination of $\tan\beta \sim 50$ as predicted by YUNS models. Finally, the predicted light higgsinos should be accessible to a linear e^+e^- collider with $\sqrt{s} \sim 0.5$ TeV.

Keywords: Supersymmetry Phenomenology, Supersymmetric Standard Model, Large Hadron Collider

*Email: baer@nhn.ou.edu

†Email: sabine.kraml@lpsc.in2p3.fr

‡Email: suchita.kulkarni@lpsc.in2p3.fr

1 Introduction

A striking feature in nature is that all the fermions of each generation fill out a complete 16-dimensional spinor multiplet of the gauge group $SO(10)$ [1]. While ordinary grand unified theories (GUTs) suffer from the notorious gauge hierarchy problem, supersymmetric (SUSY) GUTs not only tame this hierarchy problem [2], but they also receive support from the well-known unification of gauge couplings [3]. In the simplest $SO(10)$ SUSY GUT theories, where both MSSM Higgs doublets H_u and H_d occupy the same 10-dimensional representation, one also expects unification of third generation Yukawa couplings f_t , f_b and f_τ at $M_{\text{GUT}} \simeq 2 \times 10^{16}$ GeV [4, 5]. The $t - b - \tau$ Yukawa coupling unification is highly sensitive to both 2-loop renormalization group running (RGEs) and to threshold corrections when transitioning between MSSM and SM effective theories at the SUSY particle mass scale. Thus, the entire SUSY mass spectrum enters into a precise computation of Yukawa coupling unification.

Many groups have explored $t - b - \tau$ Yukawa unification (YU) in SUSY theories [6, 7, 8, 9, 10, 11, 12, 13]. It has been found that, for $\mu > 0$, YU can occur at the few percent level in either the Higgs splitting (HS) model or the DR3 model (D-term splitting, right-hand neutrino effects and third generation splitting), provided that the GUT scale soft SUSY breaking (SSB) terms are related as

$$A_0^2 \simeq 2m_{10}^2 \simeq 4m_{16}^2, \quad (1)$$

with $A_0 < 0$. Moreover, the GUT scale Higgs splitting $m_{H_u}^2 < m_{H_d}^2$ is needed to allow for an appropriate radiative breakdown of electroweak symmetry. In these models, first generation squarks and sleptons are required to be in the multi-TeV range [8, 10] while third generation sfermions are driven to much lighter TeV-scale masses. A benefit of these models is that the light SUSY Higgs boson mass m_h tends naturally to be in the 125 GeV range,¹ as required by the recent LHC discovery [16, 17]. The gaugino masses from YU SUSY are expected to be quite light, with typically $m_{\tilde{g}} \lesssim 500$ GeV (now excluded by LHC searches for gluino pair production along with cascade decay into states containing b -quarks[18]), although solutions with heavier gluinos $\sim 1 - 2$ TeV can also be found [19]. In all these cases, the superpotential μ parameter, which is extracted from the electroweak minimization conditions, occupies values in the 1–10 TeV regime, leading to severe electroweak fine-tuning (EWFT).

In this work, we examine to what extent it is possible to reconcile YU with low EWFT. Minimization of the SUSY scalar potential allows one to relate the Z mass scale to the superpartner mass scale via the well-known relation

$$\frac{1}{2}M_Z^2 = \frac{(m_{H_d}^2 + \Sigma_d) - (m_{H_u}^2 + \Sigma_u) \tan^2 \beta}{(\tan^2 \beta - 1)} - \mu^2. \quad (2)$$

The radiative corrections Σ_u and Σ_d are given in the 1-loop approximation of the Higgs effective potential by:

$$\Sigma_{u,d} = \frac{1}{v_{u,d}} \frac{\partial \Delta V}{\partial H_{u,d}}, \quad (3)$$

¹The large negative A_0 in Eq. (1) leads to maximal stop mixing, see *e.g.* [14, 15], thus increasing m_h to the desired range.

where ΔV is the one-loop correction to the tree-level potential, and the derivative is evaluated in the physical vacuum: *i.e.* the fields are set to their vacuum expectation values after evaluating the derivative. At the one-loop level and in the limit of setting first/second generation Yukawa couplings to zero, Σ_u contains 18 and Σ_d contains 19 separate contributions from various particles/sparticles [20]. We include contributions from W^\pm , Z , $\tilde{t}_{1,2}$, $\tilde{b}_{1,2}$, $\tilde{\tau}_{1,2}$, $\tilde{W}_{1,2}$, $\tilde{Z}_{1,2,3,4}$, t , b and τ , h , H and H^\pm . We adopt a scale choice $Q^2 = m_{\tilde{t}_1} m_{\tilde{t}_2}$ to minimize the largest of the logarithms. The dominant contribution to the terms $\Sigma_{u,d}$ arise from superpotential Yukawa interactions of third generation squarks involving the top quark Yukawa coupling. For instance, the dominant contribution to Σ_u is given by

$$\Sigma_u(\tilde{t}_{1,2}) = \frac{3}{16\pi^2} F(m_{\tilde{t}_{1,2}}^2) \left[f_t^2 - g_Z^2 \mp \frac{f_t^2 A_t^2 - 8g_Z^2(\frac{1}{4} - \frac{2}{3}x_W)\Delta_t}{m_{\tilde{t}_2}^2 - m_{\tilde{t}_1}^2} \right], \quad (4)$$

where $\Delta_t = (m_{\tilde{t}_L}^2 - m_{\tilde{t}_R}^2)/2 + m_Z^2 \cos 2\beta(\frac{1}{4} - \frac{2}{3}x_W)$, $g_Z^2 = (g^2 + g'^2)/8$ and $x_W \equiv \sin^2 \theta_W$ and $F(m^2) = m^2(\log \frac{m^2}{Q^2} - 1)$. This expression thus grows quadratically with the stop mass.

We adopt the fine-tuning measure from [20], which requires that each of the 40 terms on the right-hand-side (RHS) of Eq. (2) should be of order $\sim m_Z^2/2$. Labeling each term as C_i (with $i = H_d, H_u, \mu, \Sigma_d^d(\tilde{t}_1), \Sigma_u^u(\tilde{t}_1), \text{etc.}$), we may require $C_{max} \equiv \max |C_i| < \Lambda_{max}^2$, where $\Lambda_{max} \sim 100 - 300$ GeV, depending on how much EWFT one is willing to tolerate. This measure of fine-tuning is similar to (but not exactly the same as) Kitano–Nomura [21] but different from Barbieri–Giudice [22] beyond the tree-level. In the following, we will use the fine-tuning parameter

$$\Delta = C_{max}/(m_Z^2/2), \quad (5)$$

where lower values of Δ correspond to less fine-tuning, and *e.g.* $\Delta = 20$ would correspond to $\Delta^{-1} = 5\%$ fine-tuning.

Our goal in this paper is to search for parameter choices which

1. Maximize the degree of Yukawa coupling unification, i.e. minimize

$$R_{\text{yuk}} = \frac{\max(f_t, f_b, f_\tau)}{\min(f_t, f_b, f_\tau)} \quad (6)$$

with each Yukawa coupling evaluated at the GUT scale. Thus, a value of $R_{\text{yuk}} = 1$ would give perfect Yukawa coupling unification.

2. Have as low EWFT as possible (in practice, we will require $\Delta \lesssim 100$, or better than 1% EWFT).
3. Have $m_h \approx 125$ GeV in accord with the recent LHC discovery of a Higgs-like resonance. In practice, we will require $122 \text{ GeV} < m_h < 128 \text{ GeV}$ to allow for a roughly 2–3 GeV error in the RG-improved one-loop effective potential calculation of the Higgs mass m_h .

We recognize that in addition to EWFT, there also exists a fine-tuning associated with generating particular weak scale SUSY spectra from distinct GUT scale parameters [22], (see also [23, 24] for related discussions). Here we adopt the less restrictive *weak scale*

fine-tuning condition, which nonetheless turns out to be indeed very restrictive. In this vein, we regard particular GUT scale parameters as merely a parametrization of our ignorance of the mechanism of SUSY breaking and soft term generation.² For instance, in this paper we will require rather low values of superpotential μ parameter to avoid excessive EWFT in Eq. (2). In generic SUSY models, the value of μ is expected to be of order M_{Planck} since it is a dimensionful SUSY-preserving parameter. Excessively large μ can be avoided ala Giudice-Masiero [26] where the μ superpotential term is forbidden by some high scale symmetry, but then is regenerated as a soft SUSY breaking term via a Higgs–Higgs coupling to the hidden sector.

For the remainder of this paper, in Section 2 we present details of our scan over SUSY parameter space, and which constraints are invoked in our analysis. In Section 3, we present the results of our parameter space scans. We will find that requiring $\Delta \lesssim 100$ and $m_h \sim 125$ GeV only allows for R_{yuk} as low as $\sim 1.2 - 1.3$. While this degree of Yukawa unification is not optimal, we feel it is still useful in that it might guide model builders towards models including additional GUT scale threshold corrections or extra matter or above-GUT-scale running which may ameliorate the situation. In Section 5, we discuss observable consequences of YUNS for LHC, ILC and dark matter searches. We pay some attention to methods which might allow one to distinguish YUNS from generic NS models at lower $\tan\beta$ values. In Section 6 we present a summary and conclusions.

2 Parameter space and Yukawa unification

For our calculations, we adopt the ISAJET 7.83 [27] SUSY spectrum generator ISASUGRA [28]. ISASUGRA begins the calculation of the sparticle mass spectrum with input \overline{DR} gauge couplings and f_b, f_τ Yukawa couplings at the scale $Q = M_Z$ (f_t running begins at $Q = m_t$) and evolves the 6 couplings up in energy to scale $Q = M_{\text{GUT}}$ (defined as the value Q where $g_1 = g_2$) using two-loop RGEs. At $Q = M_{\text{GUT}}$, we input the soft SUSY breaking parameters as boundary conditions, and evolve the set of 26 coupled MSSM RGEs [29] back down in scale to $Q = M_Z$. Full two-loop MSSM RGEs are used for soft term evolution, while the gauge and Yukawa coupling evolution includes threshold effects in the one-loop beta-functions, so the gauge and Yukawa couplings transition smoothly from the MSSM to SM effective theories as different mass thresholds are passed. In ISASUGRA, the values of SSB terms of sparticles which mix are frozen out at the scale $Q \equiv M_{\text{SUSY}} = \sqrt{m_{\tilde{t}_L} m_{\tilde{t}_R}}$, while non-mixing SSB terms are frozen out at their own mass scale [28]. The scalar potential is minimized using the RG-improved one-loop MSSM effective potential evaluated at an optimized scale $Q = M_{\text{SUSY}}$ which accounts for leading two-loop effects [30]. Once the tree-level sparticle mass spectrum is computed, full one-loop radiative corrections are calculated for all sparticle and Higgs boson masses, including complete one-loop weak scale threshold corrections for the top, bottom and tau masses at scale $Q = M_{\text{SUSY}}$ [31]. Since the GUT scale Yukawa couplings are modified by the threshold corrections, the ISAJET RGE solution must be imposed iteratively with successive up-down running until a convergent sparticle mass solution is found. Since ISASUGRA uses a “tower of effective theories” approach to RG evolution, we expect a more accurate evaluation of the sparticle mass spectrum for models with split spectra (this

²The relation between GUT scale fine-tuning and the b – τ Yukawa coupling ratio was studied in [25].

procedure sums the logarithms of potentially large ratios of sparticle masses) than with programs which make an all-at-once transition from the MSSM to SM effective theories. The fine-tuning measure Δ described in Sec. 1 has been implemented in ISAJET 7.83 [27].

In models of “natural SUSY” (NS) [32, 21, 33, 34, 35, 36, 37, 20], the first requirement to gain a low EWFT is that the μ parameter be of the order of $\sim M_Z$, while in Yukawa-unified SUSY, it is necessary to invoke some manner of Higgs soft term splitting at the GUT scale in order to obtain radiative EWSB. For these reasons, the model parameter space chosen in this study is the two-parameter non-universal Higgs model (NUHM2) where the weak scale values of μ and m_A are input *in lieu* of the GUT scale values of $m_{H_u}^2$ and $m_{H_d}^2$. In addition, to allow for (sub)TeV-scale third generation masses (as required by EWFT from Eq. (2) along with at least a partial decoupling solution to the SUSY flavor and CP problems, we allow for split first/second and third generations at the GUT scale. Thus, the parameter space we choose is given by

$$m_{16}(1, 2), m_{16}(3), m_{1/2}, A_0, \tan \beta, \mu, m_A. \quad (7)$$

Here, $m_{16}(1, 2)$ and $m_{16}(3)$ are the first/second and third generation sfermion soft masses, respectively; $m_{1/2} \equiv M_1 = M_2 = M_3$ is the universal gaugino mass parameter; and $A_0 \equiv A_t = A_b = A_\tau$ is the universal trilinear coupling. These parameters are defined at M_{GUT} , while $\tan \beta$, μ , and m_A are defined at the weak scale. The top quark mass is set to $m_t = 173.2$ GeV.

We search for mass spectra with low EWFT Δ and low R_{yuk} by performing a vast random scan over the following parameter ranges (masses in GeV units):

$$\begin{aligned} 5000 \text{ GeV} &< m_{16}(1, 2) < 20000 \text{ GeV}, \\ 0 &< m_{16}(3) < 20000 \text{ GeV}, \\ 300 \text{ GeV} &< m_{1/2} < 2000 \text{ GeV}, \\ -2 &< A_0/m_{16}(3) < 1, \\ 50 &< \tan \beta < 60, \\ 100 \text{ GeV} &< \mu < 250 \text{ GeV}, \\ 500 \text{ GeV} &< m_A < 5000 \text{ GeV}. \end{aligned} \quad (8)$$

The lower limit on $m_{1/2}$ comes from the approximate LHC bound of $m_{\tilde{g}} \gtrsim 900$ GeV (for $m_{\tilde{q}} \gg m_{\tilde{g}}$) [38], while the lower bound on m_A comes from LHC searches for $A, H \rightarrow \tau^+ \tau^-$ which require $m_A > 500$ GeV at $\tan \beta \sim 50$ [39]. We require of our solutions that

1. electroweak symmetry be radiatively broken (REWSB),
2. the neutralino \tilde{Z}_1 is the lightest MSSM particle,
3. the light chargino mass obeys the rather model independent LEP2 limit that $m_{\tilde{W}_1} > 103.5$ GeV [40], and
4. the light Higgs mass falls within the window $m_h = 122\text{--}128$ GeV, where we adopt ± 3 GeV as theoretical error on the Higgs mass calculation.

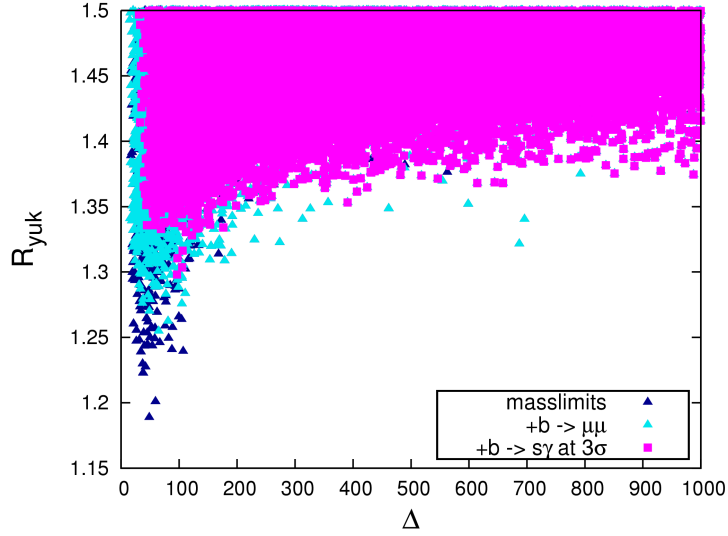


Figure 1: Scatter plot of R_{yuk} versus Δ from the scan defined in Eq. (2.2). The dark blue triangles violate the B -physics constraints of Eq. (2.3). The light blue triangles obey the $\text{BR}(B_s \rightarrow \mu^+\mu^-)$ constraint, but deviate from the measured $\text{BR}(B \rightarrow X_s\gamma)$ by more than 3σ . Finally, the pink squares satisfy both the $\text{BR}(B_s \rightarrow \mu^+\mu^-)$ and $\text{BR}(B \rightarrow X_s\gamma)$ constraints. Only points with $\Delta < 1000$ and $R_{\text{yuk}} < 1.5$ are shown.

Regarding B -physics constraints, we consider $\text{BR}(B \rightarrow X_s\gamma) = (3.55 \pm 0.34) \times 10^{-4}$, where experimental and theoretical uncertainties have been added in squares, and $\text{BR}(B_s \rightarrow \mu^+\mu^-) < 4.2 \times 10^{-9}$ at 95% CL. In the following we will impose the $\text{BR}(B \rightarrow X_s\gamma)$ constraint only at the 3σ level (the reason for this is that calculating $\text{BR}(B \rightarrow X_s\gamma)$ with both IsaTools and SuperISO, we observe deviations of the order of 5% in the relevant region of parameter space). For the $\text{BR}(B_s \rightarrow \mu^+\mu^-)$ constraint, we assume a theoretical uncertainty of 20%. This leads to the following limits

$$\begin{aligned} \text{BR}(B \rightarrow X_s\gamma) &= [2.53, 4.57] \times 10^{-4}, \\ \text{BR}(B_s \rightarrow \mu^+\mu^-) &< 5.04 \times 10^{-9}, \end{aligned} \quad (9)$$

which we will use throughout the numerical analysis.

Regarding neutralino relic density, we remark here that models of natural SUSY contain a higgsino-like lightest neutralino with thermal abundance of typically $\Omega_{\tilde{Z}_1}^{\text{TP}} h^2 \sim \mathcal{O}(10^{-3} - 10^{-2})$. This thermal under-abundance can be regarded as a positive feature of NS models in the sense that if one invokes the axion solution to the strong CP problem, then one expects mixed axion-higgsino dark matter, where the higgsino portion is typically enhanced by thermal axino production and decay to higgsinos in the early universe. Thus, a thermal under-abundance leaves room for additional non-thermal higgsino production plus an axion component to the dark matter [41].

3 Scan results

As our first result, we show in Fig. 1 points from our parameter space scan in the R_{yuk} vs. Δ plane. All points have $m_h = 122\text{--}128$ GeV and obey the current LEP and LHC SUSY

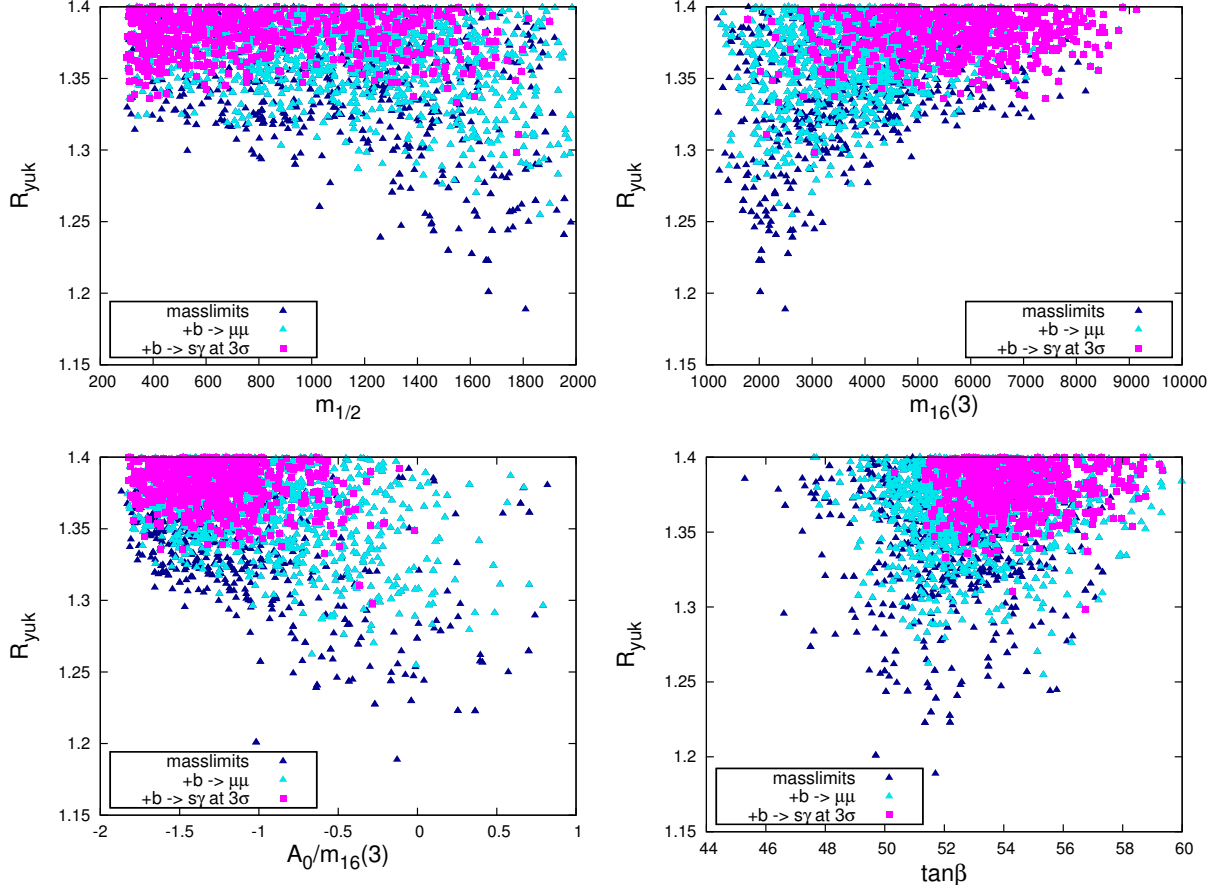


Figure 2: Dependence of R_{yuk} on $m_{1/2}$, $m_{16}(3)$, $A_0/m_{16}(3)$ and $\tan \beta$, for $\Delta < 100$. Same color code as in Fig. 1.

mass limits. The dark blue triangles however violate the B -physics constraints of Eq. (9). These points may still be valid if additional small flavor violating terms are allowed in the theory. The light blue triangles obey the $\text{BR}(B_s \rightarrow \mu^+ \mu^-)$ constraint, but deviate from the measured $\text{BR}(B \rightarrow X_s \gamma)$ by more than 3σ . Finally, the pink squares satisfy both the $\text{BR}(B_s \rightarrow \mu^+ \mu^-)$ and $\text{BR}(B \rightarrow X_s \gamma)$ constraints. This color scheme is used throughout the remainder of the paper. We see already from this plot that flavor physics constraints significantly affect the parameter space of Yukawa-unified natural SUSY. This is to be expected, since naturalness requires lighter third generation squarks while Yukawa unification requires $\tan \beta \sim 50$: both these effects bolster SUSY contributions to B -physics observables. (Analogous observations were made in [10, 42] in the context of generic YU models.) Without flavor constraints, we can obtain R_{yuk} as low as ~ 1.2 . The $\text{BR}(B_s \rightarrow \mu^+ \mu^-)$ constraint pushes this up to $R_{\text{yuk}} \gtrsim 1.27$, and the $\text{BR}(B \rightarrow X_s \gamma)$ constraint to $R_{\text{yuk}} \gtrsim 1.3$. Aside from the B -physics constraints, it is intriguing that points with lowest Δ also have lowest values of R_{yuk} . This is because low Δ requires light third generation squark masses, while at the same time Yukawa unification requires large SUSY threshold corrections which also require lighter third generation squarks.

In Fig. 2, we show the value of R_{yuk} versus various input parameters for $\Delta < 100$ (less than 1% fine-tuning). Here, the behavior deviates considerably from $t - b - \tau$ unified models with large $\mu > 0$ and a spectrum derived from the radiatively driven inverted

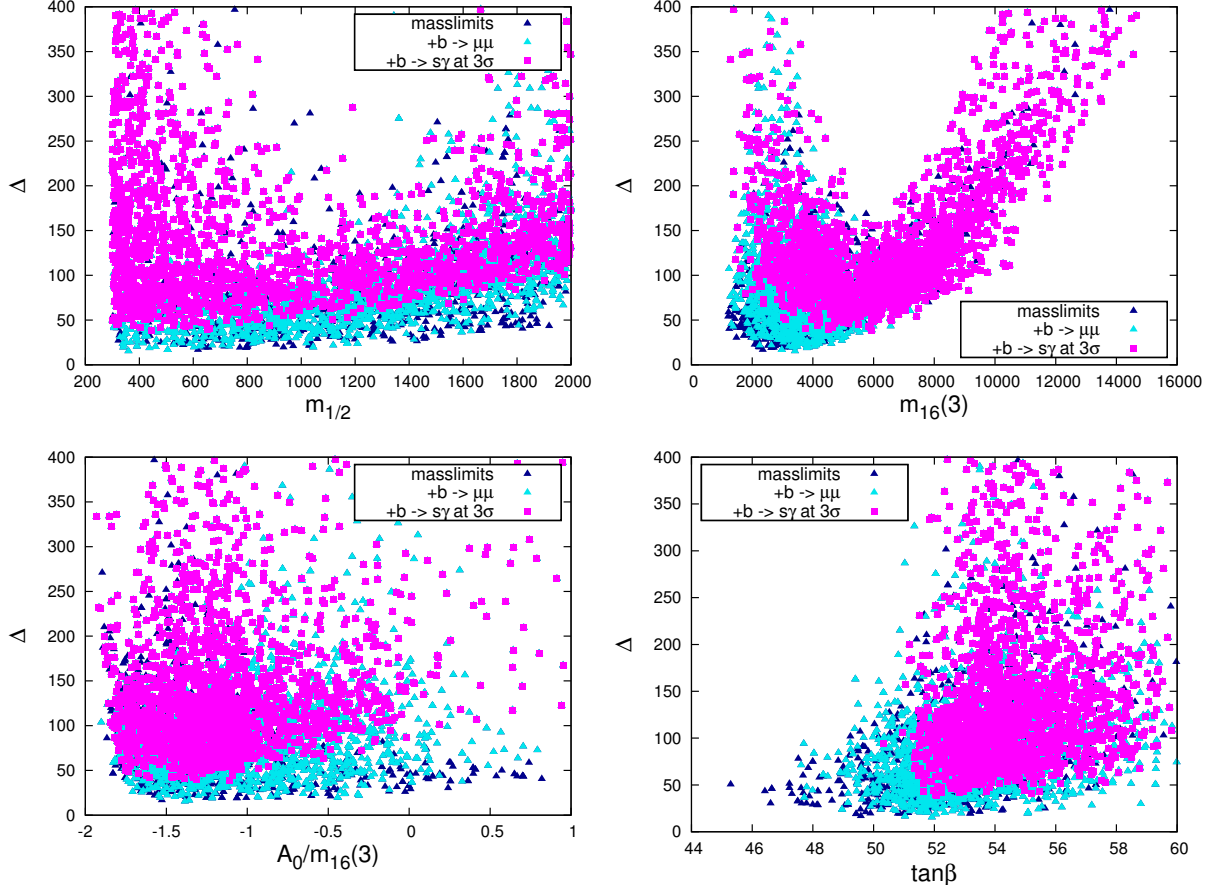


Figure 3: Dependence of fine-tuning Δ on $m_{1/2}$, $m_{16}(3)$, $A_0/m_{16}(3)$ and $\tan \beta$, for $R_{\text{yuk}} < 1.4$. Same color code as in Fig. 1.

scalar mass hierarchy [7, 8, 10]. From frame *a*), we see that YUNS models actually prefer large $m_{1/2}$ whereas generic Yukawa unified SUSY models (with $R_{\text{yuk}} \lesssim 1.1$ but arbitrary EWFT), YUS for short, prefer low $m_{1/2}$. The preference for large $m_{1/2}$ helps to avoid LHC constraints on the gluino mass. If we impose the B -physics constraints, then the distribution flattens out with some preference for lower $m_{1/2}$ values. In frame *b*), where R_{yuk} is plotted *vs.* $m_{16}(3)$, we see that lowest R_{yuk} values prefer $m_{16}(3) \sim 2$ TeV, which leads to rather light third generation squarks and typically violation of B -physics constraints. If we respect B -constraints, then larger values of $m_{16}(3) \sim 3 - 7$ TeV are preferred, at the cost of larger values of R_{yuk} . In frame *c*), we plot versus $A_0/m_{16}(3)$. For YUS models, there is a strong preference for $A_0 \sim -2m_{16}$ [7], while for YUNS, the lowest R_{yuk} values are obtained for smaller $|A_0|$. Imposing B -constraints, the preference moves to $A_0 \sim (-2 \text{ to } 0) \times m_{16}(3)$. Frame *d*) shows R_{yuk} *vs.* $\tan \beta$. As expected, $\tan \beta \sim 50$ is preferred.

The dependence of Δ on the input parameters is shown in Fig. 3 for points with $R_{\text{yuk}} < 1.4$. In frame *a*), we see a mild preference by Δ for low $m_{1/2}$, *i.e.* the gluino mass can't be too heavy, lest it pushes the stop masses too high, leading to large Σ_u . From frame *b*), we see low Δ prefers $m_{16}(3) \sim 2 - 4$ TeV. If $m_{16}(3)$ is much higher, then third generation squarks are too heavy to give low EWFT, while if $m_{16}(3)$ is too light, we generate tachyonic spectra: the optimal corresponds to $m_{16}(3) \sim 2 - 4$ TeV. For

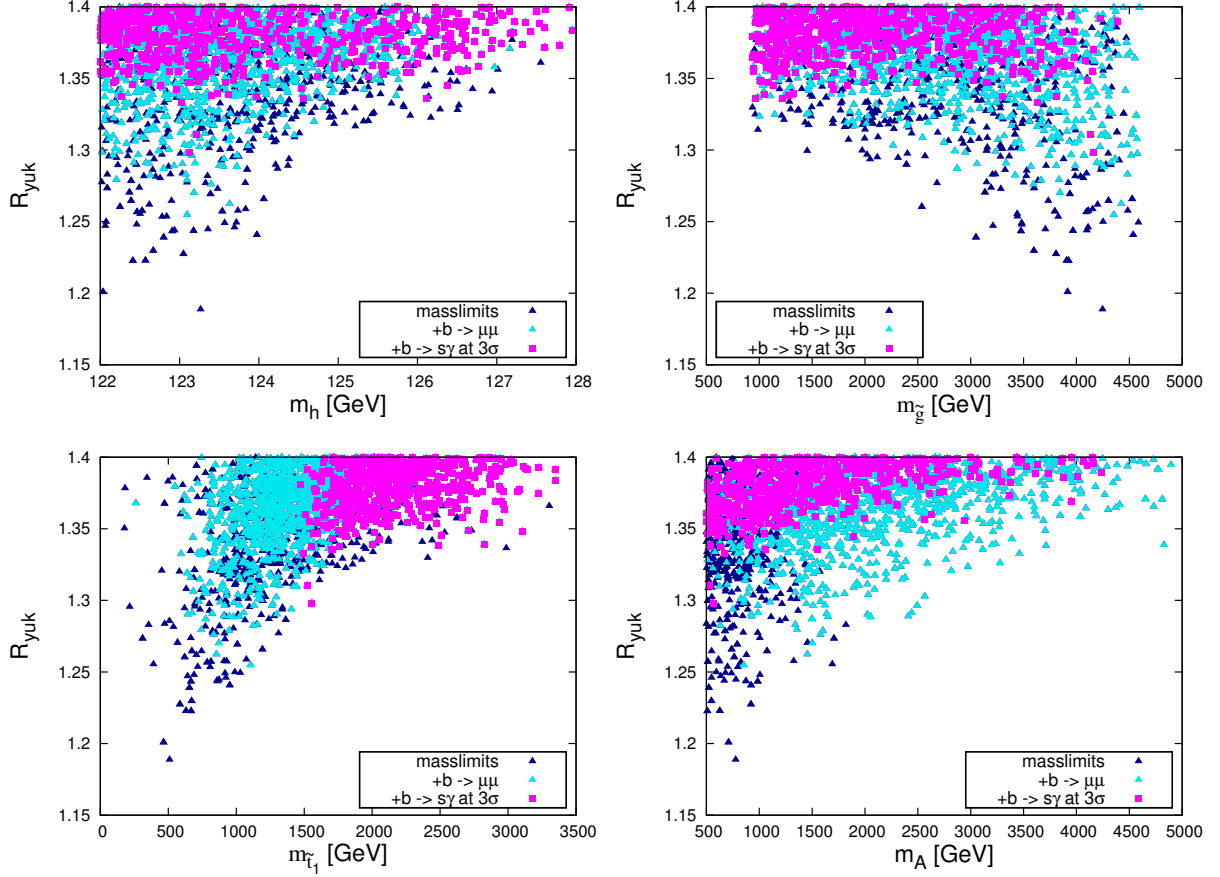


Figure 4: Dependence of R_{yuk} on m_h , $m_{\tilde{g}}$, $m_{\tilde{t}_1}$ and m_A , for $\Delta < 100$. Same color code as in Fig. 1.

$m_{16}(3) \sim 1 - 2$ TeV, then sub-TeV top squarks are generated leading to violation of B -constraints. In frame c), we see that low Δ allows a wide range of A_0 unless B -constraints are imposed, in which case $A_0 \sim (-2 \text{ to } 0) \times m_{16}(3)$ is again preferred. The large negative A_0 values lead to larger m_h values and also can lower the EWFT [24]. In frame d), we see that there is only mild preference for $\tan \beta \sim 48 - 58$ values unless B -constraints are respected, in which case $\tan \beta \gtrsim 52$ is preferred.

In Fig. 4 we show R_{yuk} versus various sparticle and Higgs masses. In frame a), the distribution versus m_h is shown, and we see that low R_{yuk} prefers the lower range of m_h . This is understandable since low EWFT prefers lower top and bottom squark masses, which may not feed a sufficient radiative correction into the m_h computation. These low third generation squark mass solutions also tend to give large contributions to B -constraint. If we impose B -constraints, then m_h can live in the 122 – 128 GeV range, at the cost of larger R_{yuk} . In frame b), we show the distribution versus $m_{\tilde{g}}$. While all solutions—especially low R_{yuk} ones—favor the heavier range of $m_{\tilde{g}}$ ($m_{\tilde{g}} \sim 2 - 5$ TeV, likely beyond LHC reach), the solutions obeying B -constraints tend to slightly favor lower $m_{\tilde{g}}$, possibly within range of LHC14 searches. In frame c), the distribution versus $m_{\tilde{t}_1}$ is shown. Here, we see a clear demarcation: B -constraints favor $m_{\tilde{t}_1} \gtrsim 1.5$ TeV to suppress SUSY loop contributions to $\text{BR}(B \rightarrow X_s \gamma)$. This constraint forces the minimum R_{yuk} to move from ~ 1.18 to about 1.3. Additional small flavor-violating contributions to the

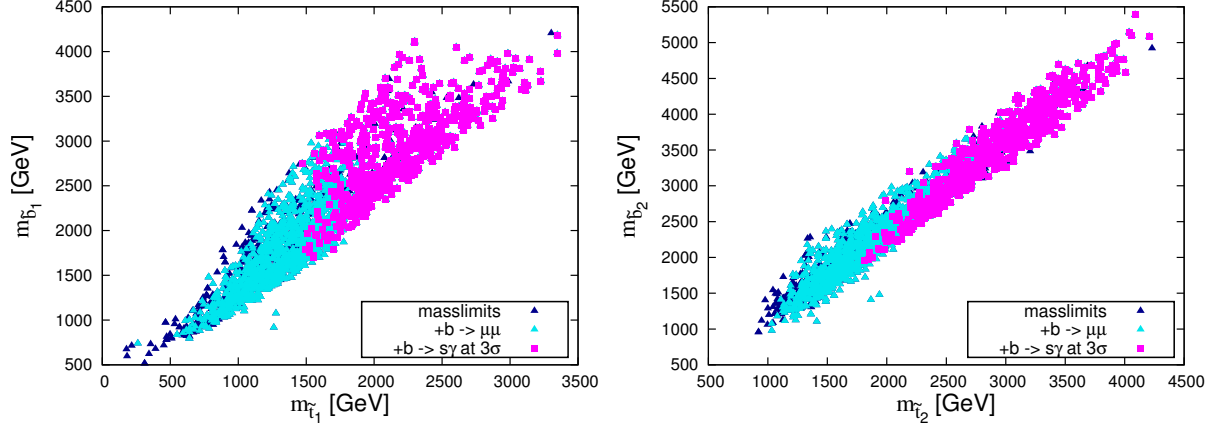


Figure 5: Distribution of scan points in a) $m_{\tilde{t}_1}$ vs. $m_{\tilde{b}_1}$ space and b) $m_{\tilde{t}_2}$ vs. $m_{\tilde{b}_2}$ space for $R_{\text{yuk}} < 1.4$ and $\Delta < 100$. Same color code as in Fig. 1.

MSSM Lagrangian could alter the predicted $\text{BR}(B \rightarrow X_s \gamma)$ and/or $\text{BR}(B_s \rightarrow \mu^+ \mu^-)$ rates and thus allow the lower R_{yuk} solutions[47]. In frame d), we show the distribution versus pseudoscalar Higgs mass m_A . We see low R_{yuk} favors the lower range of m_A , although values up to and beyond 5 TeV are also possible (at the cost of $R_{\text{yuk}} \sim 1.4$, however). Since $\tan \beta \sim 50$, LHC searches for $A, H \rightarrow \tau^+ \tau^-$ will access a significant range of m_A in this case. It is also possible for some range of $m_A \lesssim 1$ TeV for LHC to access $bA \rightarrow b\mu^+ \mu^-$ production [48].

In Fig. 5, we show scatter plots of YUNS points with $R_{\text{yuk}} < 1.4$ and $\Delta < 100$ in a) $m_{\tilde{t}_1}$ vs. $m_{\tilde{b}_1}$ and b) $m_{\tilde{t}_2}$ vs. $m_{\tilde{b}_2}$ space. From frame a), we see as expected that $m_{\tilde{t}_1}$ and $m_{\tilde{b}_1}$ are correlated, with some solutions reaching well below $m_{\tilde{t}_1} \sim 500$ GeV, which should be accessible to LHC searches. However, in this case these points all violate B -constraints, so that requiring B -constraints within measured range requires instead $m_{\tilde{t}_1}, m_{\tilde{b}_1} \gtrsim 1.5$ TeV, likely beyond the 14 TeV LHC reach. In frame b), we see also that $m_{\tilde{b}_2}$ and $m_{\tilde{t}_1}$ are correlated. This is different from usual NS, where $m_{\tilde{b}_2}$ can be far above $m_{\tilde{t}_{1,2}}$ and $m_{\tilde{b}_1}$. The reason here is that f_b is large and so there is also a non-negligible contribution to Σ_u from $\tilde{b}_{1,2}$. Imposing B -constraints, we find $m_{\tilde{t}_2}$ and $m_{\tilde{b}_2}$ both $\gtrsim 2$ TeV (the former aids in lifting m_h into its measured range).

4 Benchmark points

In this section we present several YUNS benchmark points, see Table 1, and compare to one YUS benchmark point (HSb, from the “just-so” HS model) from Ref. [43].

For HSb, $R_{\text{yuk}} \sim 1.02$, which is nearly perfect Yukawa coupling unification. The Higgs mass $m_h \simeq 127.8$ GeV is also sufficiently heavy. Unfortunately, the point is now excluded by LHC7 searches for multi-jet+ E_T^{miss} plus one b -tag searches, since $m_{\tilde{g}}$ is only 351 GeV. We also list in Table 1 the EWFT measure; for HSb we have $\Delta = 2489$, indicating exceptionally high level of fine-tuning. Much of this comes from the μ parameter which turns out to be of order 3 TeV, and thus requires a large value of $m_{H_u}^2$ at the weak scale to cancel against.

In contrast, point YUNS1 in column 3 has low fine-tuning of $\Delta = 39$, at the cost of

parameter	HSb	YUNS1	YUNS2	YUNS3
$m_{16}(1, 2)$	10000	19390.0	17149.4	19928.8
$m_{16}(3)$	10000	5938.8	2490.4	2490.5
$m_{1/2}$	43.9	444.4	1859.2	1809.1
A_0	-19947.3	-6595.5	-1374.1	-319.1
$\tan \beta$	50.398	52.09	54.2	51.7
μ	3132.6	136.0	106.1	169.6
m_A	1825.9	884.1	541.2	776.4
f_t	0.557	0.578	0.563	0.549
f_b	0.557	0.423	0.474	0.496
f_τ	0.571	0.561	0.618	0.590
R_{yuk}	1.025	1.37	1.3	1.19
Δ	2489	39	105	48
$m_{\tilde{g}}$	351.2	1328.5	4309.5	4247.2
$m_{\tilde{u}_L}$	9972.1	19396.8	17466.6	20189.0
$m_{\tilde{t}_1}$	2756.5	1587.3	1598.0	509.3
$m_{\tilde{b}_1}$	3377.1	2176.3	1857.1	793.1
$m_{\tilde{e}_R}$	10094.7	19379.3	17153.2	19930.2
$m_{\tilde{W}_1}$	116.4	137.3	112.5	177.4
$m_{\tilde{Z}_2}$	113.8	147.4	112.0	176.2
$m_{\tilde{Z}_1}$	49.2	118.9	106.2	170.3
m_h	127.8	123.1	123.8	123.3
$\text{BR}(B \rightarrow X_s \gamma)$	3.1×10^{-4}	2.7×10^{-4}	2.8×10^{-4}	2.4×10^{-4}
$\text{BR}(B_s \rightarrow \mu^+ \mu^-)$	8.1×10^{-9}	4.5×10^{-9}	4.6×10^{-9}	2.4×10^{-8}
$\Omega_{\tilde{Z}_1}^{\text{TP}} h^2$	4613	0.01	0.004	0.007
$\sigma^{\text{SI}}(\tilde{Z}_1 p)$ pb	2.2×10^{-13}	4.5×10^{-8}	4.7×10^{-9}	2.9×10^{-9}
$\sigma^{\text{SD}}(\tilde{Z}_1 p)$ pb	1.2×10^{-9}	7.3×10^{-4}	3.6×10^{-5}	1.6×10^{-5}
$\langle \sigma v \rangle _{v \rightarrow 0}$ cm ³ /s	1.9×10^{-32}	2.4×10^{-25}	3.3×10^{-25}	2.8×10^{-25}

Table 1: Parameters and masses in GeV units for HSb [43] and three Yukawa-unified natural SUSY (YUNS) benchmark points. We also show B -decay constraints and dark matter relic density and (in)direct detection cross sections.

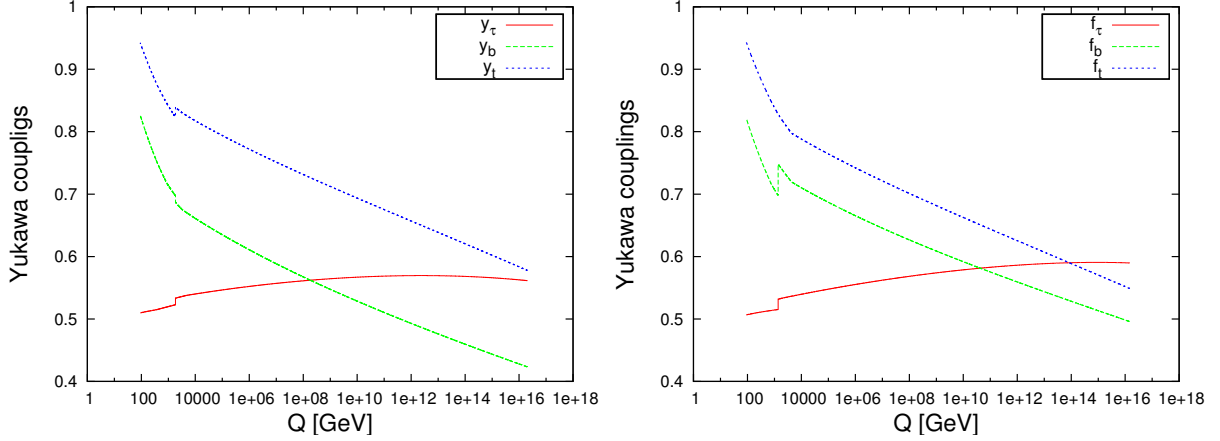


Figure 6: Evolution of Yukawa couplings for benchmark points YUNS1 (left) and YUNS3 (right) versus renormalization scale Q .

relaxing R_{yuk} to 1.37. For YUNS1, $m_{\tilde{g}} \simeq 1.3$ TeV, with first/second generation squarks at ~ 19 TeV. The point is likely beyond LHC8 reach, but should be accessible to LHC14 with $10\text{--}100\text{ fb}^{-1}$. In column 4, we list YUNS2 with $R_{\text{yuk}} = 1.3$, as low as allowed by B -constraints, but with $\Delta \sim 100$. This point has $m_{\tilde{g}} \sim 4.3$ TeV and $m_{\tilde{q}} \sim 17.5$ TeV, so it is likely beyond LHC reach, including a high-luminosity upgrade. While the higgsino-like chargino is only 112.5 GeV, it decays via 3-body mode into a higgsino-like \tilde{Z}_1 with $m_{\tilde{Z}_1} = 106.2$ GeV, so that visible decay products are very soft, and likely impossible to observe above SM backgrounds at the LHC. Point YUNS3, listed in column 5, features R_{yuk} as low as 1.19, with $\Delta = 48$. This point has $\text{BR}(B \rightarrow X_s \gamma) = 2.4 \times 10^{-4}$, and $\text{BR}(B_s \rightarrow \mu^+ \mu^-) = 2.4 \times 10^{-8}$, so it falls out of the B -physics allowed range. While gluinos and first/second generation squarks are beyond LHC reach, the rather light top and bottom squarks may be accessible to LHC searches. All these points have $\Omega_{\tilde{Z}_1} h^2 \ll 0.11$, leaving room for non-thermal higgsino production and axions. This contrasts point HSb, which has a much too thermal abundance and so would need an extremely light axino or huge late-time entropy production to tame this over-abundance [41].

In Fig. 6, we show the Yukawa coupling evolution of f_t , f_b and f_τ versus renormalization group scale Q , from m_{weak} to M_{GUT} for benchmark points YUNS1 and YUNS3. These can be compared to similar plots for YUS, as in *e.g.* Fig. 6 of Ref. [44]. The SUSY threshold corrections implemented at the scale $Q = \sqrt{m_{\tilde{t}_1} m_{\tilde{t}_2}}$ show up as jumps in the curves. In the case of YUS models, the m_b threshold correction is positive due to a large $\tilde{t}_i \tilde{W}_j$ loop contribution which goes like $\delta_b \sim (f_t^2/32\pi^2)(\mu A_t/m_{\tilde{t}}^2) \tan \beta$, where both μ and A_t are extremely large. For YUNS models, with rather low μ , these loops are suppressed and in the case of YUNS1, the $\tilde{g} \tilde{b}_i$ loops actually dominate, and are of opposite sign to the $\tilde{t}_i \tilde{W}_j$ loops, leading to the slight downward jump of f_b and thus bad Yukawa coupling unification. For YUNS3, the $\tilde{t}_i \tilde{W}_j$ loops are larger, and the jump goes upwards, thus providing better Yukawa coupling unification.

5 Yukawa-unified natural SUSY: LHC, ILC and DM searches

In this Section, we discuss the observable consequences of YUNS for LHC, ILC and direct and indirect WIMP and also axion searches.

5.1 YUNS at LHC

In natural SUSY models, it is favorable to have multi-TeV first/second generation squarks and sleptons because 1. they are safely beyond current LHC searches, 2. they provide at least a partial solution to the SUSY flavor and CP problems and 3. they provide additional suppression of third generation scalar masses via large 2-loop RGE effects. However, this means they are likely beyond any conceivable LHC reach. Third generation squarks may be much lighter, and in generic NS models are naively expected to be below the TeV scale (but see Ref. [24] where 1–4 TeV third generation squarks work just fine, and lift the value of m_h into its measured range). In the case of YUNS, with $\tan\beta \sim 50$, the combined light squarks and large $\tan\beta$ usually imply violation of B -constraints, and if these are imposed, then top and bottom squarks are beyond 1.5 TeV, and likely inaccessible to LHC searches. If additional sources of flavor violation are invoked, then the B -constraints may be invalid, and then the solutions with much lower $R_{\text{yuk}} \sim 1.2$ are accessible, along with much lighter top and bottom squarks, potentially accessible to LHC searches.

For YUNS, the gluino mass may lie anywhere in the 1–5 TeV range. It has been estimated in Ref. [45] that LHC14 with 100 fb^{-1} should be able to access gluino pair production in the case of heavy squarks for $m_{\tilde{g}}$ up to 1.8 TeV. In the case of YUNS with heavier top and bottom squarks, the \tilde{g} is expected to dominantly decay via 3-body modes into $t\bar{t}\tilde{Z}_i$ and $t\bar{b}\tilde{W}_i$ final states. The gluino pair events will thus contain multi-jets plus missing energy plus isolated leptons plus several identifiable b -jets [46]. While the higgsino-like chargino and neutralino production cross sections can be large, their decays to soft visible particles, arising from the small energy release in their 3-body decays, will be difficult to detect at LHC above SM backgrounds [35].

In the case where $m_A \lesssim 1 \text{ TeV}$, then it may be possible to detect A , $H \rightarrow \tau^+\tau^-$, especially if these are produced in association with b -jets, *e.g.* $pp \rightarrow bA$, bH production. It may also be possible to detect bA , bH production with $A, H \rightarrow \mu^+\mu^-$ [48], since the production and decay are enhanced at large $\tan\beta$. In this case, the A , H mass and width may be determined by reconstructing $m(\mu^+\mu^-)$. At large $\tan\beta$, this width is typically in the tens of GeV range and is very sensitive to $\tan\beta$. This reaction offers a method to distinguish YUNS from NS, in that the former is expected to occur at $\tan\beta \sim 50$.

5.2 YUNS at ILC

A linear e^+e^- collider operating at $\sqrt{s} \sim 250 - 500 \text{ GeV}$ would in many ways be an optimal discovery machine for YUNS. The reason is that by construction $\mu \lesssim 250 \text{ GeV}$, so chargino and neutralino pair production should always be available. While the small energy release in \tilde{W}_1 and \tilde{Z}_2 decay is problematic at LHC, it should be much more easily observable in the clean environment of an e^+e^- collider. In this sense, an e^+e^- collider operating at $\sqrt{s} \sim 250 - 500 \text{ GeV}$ would be a higgsino in addition to a Higgs factory. It is

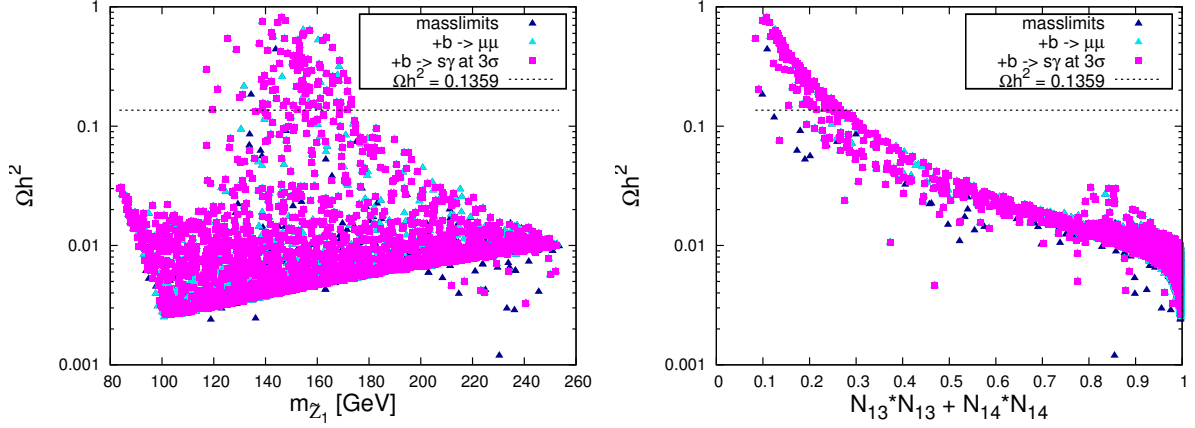


Figure 7: Thermal neutralino relic density Ωh^2 versus \tilde{Z}_1 mass (left) and versus \tilde{Z}_1 higgsino fraction (right) for scan points with $R_{\text{yuk}} < 1.4$ and $\Delta < 100$. Same color code as in Fig. 1.

also possible that some lighter third generation squarks are accessible to ILC with $\sqrt{s} \sim 1$ TeV or CLIC with $\sqrt{s} = 3$ TeV, depending if one avoids B -constraints and accepts the low mass, low R_{yuk} solutions.

5.3 Higgsino-like WIMPs

A generic prediction of both NS and YUNS models is that the LSP is a higgsino-like WIMP with a typical under-abundance of thermally produced (TP) neutralinos $\Omega_{\tilde{Z}_1}^{\text{TP}} h^2 \sim 0.002 - 0.01$. However, in cases where $m_{1/2}$ is as low as ~ 300 GeV and μ is as large as $200 - 250$ GeV, then there can be substantial bino-higgsino mixing, boosting $\Omega_{\tilde{Z}_1}^{\text{TP}} h^2$ up to 0.11 or even beyond. The situation is illustrated in Fig. 7, where we plot $\Omega_{\tilde{Z}_1}^{\text{TP}} h^2$ versus $m_{\tilde{Z}_1}$ and versus the \tilde{Z}_1 higgsino fraction from YUNS models satisfying $R_{\text{yuk}} < 1.4$ and $\Delta < 100$.

The typical under-abundance is an appealing feature if one invokes the Peccei-Quinn solution to the strong CP problem, in which case one must introduce an axion superfield \hat{a} which contains a pseudoscalar axion a as well as a spin-1/2 axino \tilde{a} and a spin-0 saxion s . In such models, one expects both saxion and axino masses at or around the SUSY breaking scale, so that dark matter is comprised of an axion-WIMP admixture. In this case, thermal production of axinos and subsequent decay to states such as $\tilde{a} g$ bolster the WIMP abundance beyond its TP-value. In addition, axions are produced as usual via coherent oscillations. It is also possible to suppress the WIMP abundance in the mixed $a\tilde{Z}_1$ cosmology via late-time entropy production from saxion production and decay, although this case tends to be highly constrained by maintaining successful Big Bang nucleosynthesis (BBN). The upshot is that in the mixed $a\tilde{Z}_1$ dark matter scenario, it may be possible to detect both a WIMP and an axion.

In the case of the YUNS model, the higgsino-like neutralinos have a substantial spin-independent (SI) direct detection cross section, as illustrated in Table 1, where $\sigma^{\text{SI}}(\tilde{Z}_1 p) \sim 10^{-8}$ pb. While this level of direct detection cross section is now highly constrained by recent XENON100 [49] results, one must bear in mind that the higgsino-like WIMPs would constitute only a portion of the dark matter, so their local abundance might be

up to a factor of 30 lower than is commonly assumed. In Table 1, we also list $\sigma^{\text{SD}}(\tilde{Z}_1 p)$ (relevant for WIMP detection at IceCube) and $\langle\sigma v\rangle|_{v\rightarrow 0}$, relevant for detection of dark matter annihilation into gamma rays or anti-matter throughout the cosmos. While these cross sections are also at potentially observable levels, again one must take into account that the overall WIMP abundance may be up to a factor of about 30 below what is commonly assumed. Plots of $\sigma^{\text{SI}}(\tilde{Z}_1 p)$, $\sigma^{\text{SD}}(\tilde{Z}_1 p)$ and $\langle\sigma v\rangle|_{v\rightarrow 0}$ have been presented in the case of higgsino-like WIMPs in Ref's [35] and [37] and so similar plots will not be reproduced here.

6 Summary and conclusions

Previous analyses of $t - b - \tau$ Yukawa-unified models suffer from two problems: 1. they tend to predict a light gluino $m_{\tilde{g}} \lesssim 500$ GeV (although solutions are possible for much heavier gluinos) which is now excluded by LHC searches, and 2. they suffer from extreme fine-tuning in the electroweak sector. In this paper, we examined how well the Yukawa couplings could unify in the natural SUSY context, where $\mu \sim 100 - 250$ GeV, while at the same time requiring the light Higgs mass $m_h \sim 122 - 128$ GeV. The small value of μ suppresses the large $\tilde{t}_i \tilde{W}_j$ loop contributions to the b -quark Yukawa coupling which seem to be needed for precision Yukawa coupling unification. Nonetheless, by scanning over NUHM2 parameters with split third generation, we are able to find solutions with R_{yuk} as low as 1.18. These solutions, with very light third generations squarks and $\tan\beta \sim 50$ tend to violate B -physics constraints. If B -physics constraints are imposed, then only $R \sim 1.3$ can be achieved. However, the B -physics calculations can be modified if additional small flavor-violating terms are allowed in the MSSM Lagrangian, so it is not clear how seriously $R \gtrsim 1.3$ should be taken.

The Yukawa-unified natural SUSY spectra have important differences from previous YU spectra. The gluino mass can easily be in the 1–4 TeV range, thus avoiding LHC constraints from SUSY searches. The light higgsino-like charginos and neutralinos decay to soft particles, also avoiding LHC searches. However, light higgsinos should be easily accessible to an ILC with $\sqrt{s} \sim 0.25 - 05$ TeV, as is typical of all NS models. In addition, as in all NS models, the lightest neutralino is higgsino-like with a typical thermal underabundance of WIMP dark matter. We regard this as a positive feature in that the WIMP abundance is typically increased in non-standard (but more attractive) cosmologies such as those containing mixed axion-neutralino cold dark matter.

The question arises as to how to distinguish YUNS from ordinary NS. The YUNS model requires $\tan\beta \sim 50$, which leads to large production cross sections for heavy Higgs bosons A and H at LHC, and large widths for these particles. If the rare decays $A, H \rightarrow \mu^+ \mu^-$ can be identified with sufficiently high statistics (perhaps at a luminosity upgraded LHC), then the widths may be measured with precision, allowing one to highly constrain $\tan\beta$, and perhaps verify that it is consistent with YUNS models.

Acknowledgments

This work has been supported in part by the Office of Science, US Department of Energy and by IN2P3 under contract PICS FR–USA No. 5872. HB and SK acknowledge the

hospitality of the Aspen Center for Physics which is supported by the National Science Foundation Grant No. PHY-1066293.

References

- [1] H. Georgi, in *Proceedings of the American Institute of Physics*, edited by C. Carlson (1974); H. Fritzsch and P. Minkowski, *Ann. Phys.* **93**, 193 (1975); M. Gell-Mann, P. Ramond and R. Slansky, *Rev. Mod. Phys.* **50**, 721 (1978); for reviews, see *e.g.* R. Mohapatra, hep-ph/9911272 (1999) and S. Raby, in *Rept. Prog. Phys.* **67** (2004) 755.
- [2] E. Witten, *Nucl. Phys.* **B188** (1982) 513; R. Kaul, *Phys. Lett.* **B109** (1982) 19.
- [3] S. Dimopoulos, S. Raby and F. Wilczek, *Phys. Rev.* **D24** (1981) 1681; M. Einhorn and D.R.T. Jones, *Nucl. Phys.* **B196** (1982) 475; W. Marciano and G. Senjanovic, *Phys. Rev.* **D25** (1982) 3092; U. Amaldi, W. de Boer and H. Furstenau, *Phys. Lett.* **B260** (1991) 447; J. Ellis, S. Kelley and D. V. Nanopoulos, *Phys. Lett.* **B260** (1991) 131; P. Langacker and Luo, *Phys. Rev.* **D44** (1991) 817.
- [4] B. Ananthanarayan, G. Lazarides and Q. Shafi, *Phys. Rev.* **D44** (1991) 1613 and *Phys. Lett.* **B300** (1993) 245; G. Anderson *et al.* *Phys. Rev.* **D47** (1993) 3702 and *Phys. Rev.* **D49** (1994) 3660; V. Barger, M. Berger and P. Ohmann, *Phys. Rev.* **D49** (1994) 4908; M. Carena, M. Olechowski, S. Pokorski and C. Wagner, *Nucl. Phys. B* **426** (1994) 269; B. Ananthanarayan, Q. Shafi and X. Wang, *Phys. Rev.* **D50** (1994) 5980; R. Rattazzi and U. Sarid, *Phys. Rev.* **D53** (1996) 1553; T. Blazek, M. Carena, S. Raby and C. Wagner, *Phys. Rev.* **D56** (1997) 6919; T. Blazek and S. Raby, *Phys. Lett.* **B392** (1997) 371; T. Blazek and S. Raby, *Phys. Rev.* **D59** (1999) 095002; T. Blazek, S. Raby and K. Tobe, *Phys. Rev.* **D60** (1999) 113001 and *Phys. Rev.* **D62** (2000) 055001; S. Profumo, *Phys. Rev.* **D68** (2003) 015006; C. Pallis, *Nucl. Phys.* **B678** (2004) 398; M. Gomez, G. Lazarides and C. Pallis, *Phys. Rev.* **D61** (2000) 123512, *Nucl. Phys.* **B638** (2002) 165 and *Phys. Rev.* **D67** (2003) 097701; U. Chattopadhyay, A. Corsetti and P. Nath, *Phys. Rev.* **D66** (2002) 035003; M. Gomez, T. Ibrahim, P. Nath and S. Skadhauge, *Phys. Rev.* **D72** (2005) 095008.
- [5] Some recent work includes: M. Badziak and K. Sakurai, *JHEP***1202** (2012) 125; M. Badziak, *Mod. Phys. Lett. A* **27** (2012) 1230020; A. S. Joshipura and K. M. Patel, arXiv:1206.3910; I. Gogoladze, Q. Shafi and C. S. Un, *JHEP***1207** (2012) 055
- [6] H. Baer, M. Diaz, J. Ferrandis and X. Tata, *Phys. Rev.* **D61** (2000) 111701; H. Baer, M. Brhlik, M. Diaz, J. Ferrandis, P. Mercadante, P. Quintana and X. Tata, *Phys. Rev.* **D63** (2001) 015007.
- [7] H. Baer and J. Ferrandis, *Phys. Rev. Lett.* **87** (2001) 211803.
- [8] D. Auto, H. Baer, C. Balazs, A. Belyaev, J. Ferrandis and X. Tata, *JHEP***0306** (2003) 023.

- [9] T. Blazek, R. Dermisek and S. Raby, Phys. Rev. Lett. **88** (2002) 111804; T. Blazek, R. Dermisek and S. Raby, Phys. Rev. **D65** (2002) 115004; R. Dermisek, S. Raby, L. Roszkowski and R. Ruiz de Austri, JHEP**0304** (2003) 037; R. Dermisek, S. Raby, L. Roszkowski and R. Ruiz de Austri, JHEP**0509** (2005) 029.
- [10] H. Baer, S. Kraml, S. Sekmen and H. Summy, JHEP**0810** (2008) 079.
- [11] W. Altmannshofer, D. Guadagnoli, S. Raby and D. Straub, Phys. Lett. **B668** (2008) 385.
- [12] I. Gogoladze, R. Khalid, S. Raza and Q. Shafi, JHEP**1012** (2010) 055 and JHEP**1106** (2011) 117.
- [13] G. Elor, L. J. Hall, D. Pinner and J. T. Ruderman, arXiv:1206.5301.
- [14] H. Baer, V. Barger and A. Mustafayev, arXiv:1112.3017.
- [15] F. Brummer, S. Kraml and S. Kulkarni, arXiv:1204.5977.
- [16] G. Aad *et al.* [ATLAS Collaboration], arXiv:1207.7214.
- [17] S. Chatrchyan *et al.* [CMS Collaboration], arXiv:1207.7235.
- [18] G. Aad *et al.* [ATLAS Collaboration], Phys. Rev. D **85** (2012) 112006.
- [19] H. Baer, S. Raza and Q. Shafi, Phys. Lett. **B712** (2012) 250.
- [20] H. Baer, V. Barger, P. Huang, A. Mustafayev and X. Tata, arXiv:1207.3343.
- [21] R. Kitano and Y. Nomura, Phys. Lett. **B631** (2005) 58 and Phys. Rev. **D73** (2006) 095004.
- [22] R. Barbieri and G. F. Giudice, Nucl. Phys. **B306** (1988) 63.
- [23] D. M. Ghilencea, H. M. Lee and M. Park, JHEP**1207** (2012) 046.
- [24] C. Wymant, arXiv:1208.1737.
- [25] S. Antusch, L. Calibbi, V. Maurer, M. Monaco and M. Spinrath, Phys. Rev. **D85** (2012) 035025 and arXiv:1207.7236.
- [26] G. F. Giudice and A. Masiero, Phys. Lett. **B206** (1988) 480.
- [27] ISAJET, by H. Baer, F. Paige, S. Protopopescu and X. Tata, hep-ph/0312045.
- [28] H. Baer, C. H. Chen, R. Munroe, F. Paige and X. Tata, Phys. Rev. **D51** (1995) 1046; H. Baer, J. Ferrandis, S. Kraml and W. Porod, Phys. Rev. **D73** (2006) 015010.
- [29] S. Martin and M. Vaughn, Phys. Rev. **D50** (1994) 2282.
- [30] H. Haber and R. Hempfling, Phys. Rev. **D48** (1993) 4280.

- [31] R. Hempfling, Phys. Rev. **D49** (1994) 6168; L. J. Hall, R. Rattazzi and U. Sarid, Phys. Rev. **D50** (1994) 7048; M. Carena *et al.*, Nucl. Phys. **B426** (1994) 269; D. Pierce, J. Bagger, K. Matchev and R. Zhang, Nucl. Phys. **B491** (1997) 3.
- [32] K. L. Chan, U. Chattopadhyay and P. Nath, Phys. Rev. **D58** (1998) 096004.
- [33] H. Baer, S. Kraml, A. Lessa, S. Sekmen and X. Tata, JHEP**1010** (2010) 018.
- [34] M. Asano, H. D. Kim, R. Kitano and Y. Shimizu, JHEP**1012** (2010) 019.
- [35] H. Baer, V. Barger and P. Huang, JHEP**1111** (2011) 031.
- [36] M. Papucci, J. T. Ruderman and A. Weiler, arXiv:1110.6926; C. Brust, A. Katz, S. Lawrence and R. Sundrum, JHEP**1203** (2012) 103.
- [37] H. Baer, V. Barger, P. Huang and X. Tata, JHEP**1205** (2012) 109.
- [38] G. Aad *et al.* [ATLAS Collaboration], arXiv:1208.0949; S. Chatrchyan *et al.* [CMS Collaboration], arXiv:1207.1798;
- [39] S. Chatrchyan *et al.* [CMS Collaboration], Phys. Lett. **B713** (2012) 68.
- [40] Joint LEP 2 Supersymmetry Working Group, *Combined LEP Chargino Results up to 208 GeV*,
http://lepsusy.web.cern.ch/lepsusy/www/inos_moriond01/charginos_pub.html.
- [41] H. Baer, A. Lessa and W. Sreethawong, JCAP **1201**, 036 (2012).
- [42] M. Albrecht, W. Altmannshofer, A. J. Buras, D. Guadagnoli and D. M. Straub, JHEP**0710** (2007) 055.
- [43] H. Baer, M. Haider, S. Kraml, S. Sekmen and H. Summy, JCAP **0902** (2009) 002.
- [44] H. Baer, S. Kraml and S. Sekmen, JHEP**0909** (2009) 005.
- [45] H. Baer, X. Tata and J. Woodside, Phys. Rev. **D45** (1992) 142; H. Baer, C. H. Chen, F. Paige and X. Tata, Phys. Rev. **D52** (1995) 2746 and Phys. Rev. **D53** (1996) 6241; H. Baer, C. H. Chen, M. Drees, F. Paige and X. Tata, Phys. Rev. **D59** (1999) 055014, H. Baer, C. Balázs, A. Belyaev, T. Krupovnickas and X. Tata, JHEP**0306** (2003) 054; see also, S. Abdullin and F. Charles, Nucl. Phys. **B547** (1999) 60; S. Abdullin *et al.* (CMS Collaboration), J. Phys. **G28** (2002) 469 [hep-ph/9806366]; B. Allanach, J. Hetherington, A. Parker and B. Webber, JHEP**08** (2000) 017.
- [46] H. Baer, X. Tata and J. Woodside, Phys. Rev. **D42** (1990) 1568.
- [47] F. Gabbiani, E. Gabrielli, A. Masiero and L. Silvestrini, Nucl. Phys. **B477** (1996) 321.
- [48] H. Baer, A. Belyaev, C. Kao and P. Svantesson, Phys. Rev. **D84** (2011) 095029.
- [49] XENON100 Collaboration, arXiv:1207.5988.